DOI: 10.53469/jtpes.2024.04(01).15

A Self-Guided Deep Learning Technique for MRI Image Noise Reduction

Xu Yan[1,*], MingXuan Xiao[2], Weimin Wang[3], Yufeng Li[4], Fei Zhang[5]

[1]Department of Computer and Science, Trine University, Phoenix 85201, US
[2]Department of Computer and Science, SouthWest JiaoTong University, Chengdu 610000, China
[3]Department of Computer and Science, Hong Kong University of Science and Technology, Hong Kong 999077, Hong Kong
[4]Department of Computer and Science, University of Southampton, Southampton SO19, UK
[5]Department of Computer and Science, Trine University, Phoenix 85201, US
**Correspondence Author*

Abstract: ***In recent years, methods founded on deep learning have exhibited notable efficacy within the field of medical image denoising. However, the majority of deep learning approaches typically require paired training data, which poses challenges for clinical diagnoses of conditions such as novel coronavirus pneumonia. This paper introduces an unsupervised learning methodology for denoising magnetic resonance images (MRI). Firstly, we employ content encoders and random noise encoders to separate the content information and noise artifacts from low-quality MRI images affected by noise. Secondly, we regularize the noise distribution through Kullback-Leibler (KL) divergence loss. Thirdly, an adversarial loss is incorporated into the model to augment the realism of the generated denoised images. Finally, we incorporate cycle consistency and perceptual losses to ensure the coherence of content information between noisy input and denoised output images. The effectiveness of the proposed approach is substantiated by experimental results, showcasing significant enhancements in visual quality.***

Keywords: MRI Denoising, Rician Noise, Unsupervised Deep Learning, Disentangled Representations.

1. INTRODUCTION

MRI images are cross-sectional images that display anatomical and pathological structures with varying grayscale intensities. They are widely used in disease detection, diagnosis, and treatment monitoring. However, the imaging process of MRI often introduces random noise, resulting in the production of low-quality MRI images. The quality of MRI images not only impacts a physician's assessment of a patient's condition but also reduces the accuracy of tasks. Image denoising can enhance the quality of a given image and address image degradation caused by random noise.

To remove noise while preserving the integrity of image content, researchers have proposed classical spatial pixel feature denoising algorithms such as Gaussian filtering, bilateral filtering, and arithmetic mean filtering[1]. In contrast to these methods that utilize local image information, non-local means denoising algorithms utilize information from the entire image. In 2008, Jose and colleagues successfully applied an improved algorithm for MRI image denoising[2]. Transform domain denoising algorithms involve first transforming the image domain and then applying denoising techniques indirectly. Dabov and others combined the calculation of similar blocks means algorithm with denoising methods in the wavelet transform domain, resulting in the BM3D algorithm[3]. Building upon the BM3D algorithm, Eksioglu and colleagues proposed an MRI reconstruction algorithm[4]. Additionally, the low-rank constraint of image matrices is noteworthy[5] [6]. Zhang Yuhan and others proposed a magnetic resonance image denoising model that combines low-rank constraints and sparse gradient priors[7].

Significant strides have been made by convolutional neural networks in the realm of image recognition [8] [9]. Consequently, there is a growing interest among researchers in image denoising algorithms grounded in convolutional neural networks[10] [11]. Among them, methods such as DnCNN [10] [12], PRI-PB-CNN [13], and MIFCN [14] exhibit strong scalability, providing excellent denoising results not only for natural images but also for MRI image denoising.

Generative adversarial networks (GANs) have demonstrated substantial advantages in the generation of realistic images[15] [16]. Consequently, researchers have combined GANs with convolutional neural networks for image denoising[17]. Most mainstream denoising algorithms fall within the supervised domain, requiring paired training data[18] [19]. However, obtaining paired data for model training is challenging in real-life scenarios. Transfer learning is a widely used approach in medical image analysis[20], and researchers like Lu Siyuan have applied it to medical image detection[21]. In cases where training data is not paired, we also utilize transfer learning to train our model.

We propose an image denoising theory based on deep learning[22] to obtain high-quality natural and MRI images. The primary contributions of this paper can be summarized as follows: 1) We introduce an learning method based on denoising, eliminating the need for paired training data; 2) We employ a disentangled representation to separate the content information from noise in low-quality MRI images[23].

2. METHODOLOGY

This model consists of the following parts, as shown in Figure 1: 1) Content encoder ECL in the low-quality images affected by random noise; content encoder ECH for the high-quality image domain; 2) Random noise encoder EN; 3) Low-quality DL and high-quality DH; 4) Low-quality generator of images GL and high-quality GH. In addition, the sample data, as shown in Figure 2, where sample l L pertains to the low-quality; sample h H pertains to the domain of high-quality; ZN=En l is the distribution of noise features.

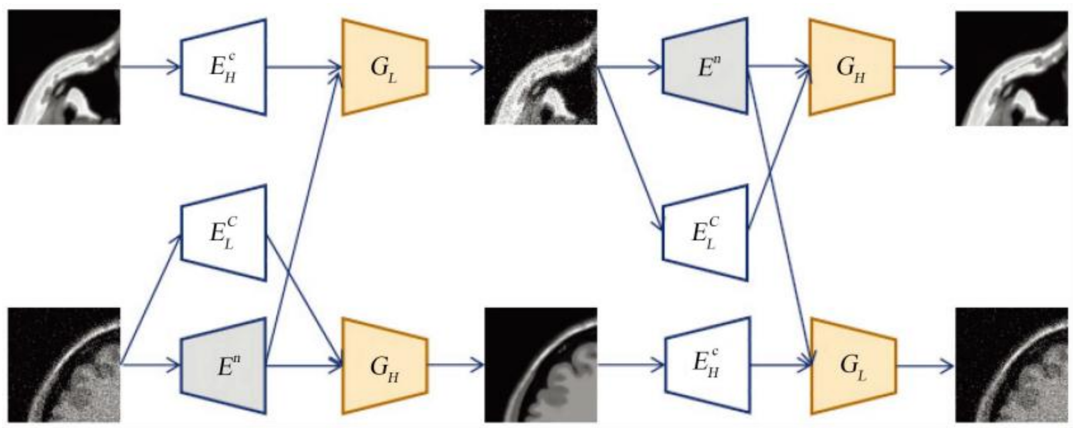

Figure 1: Overview of the denosing framework

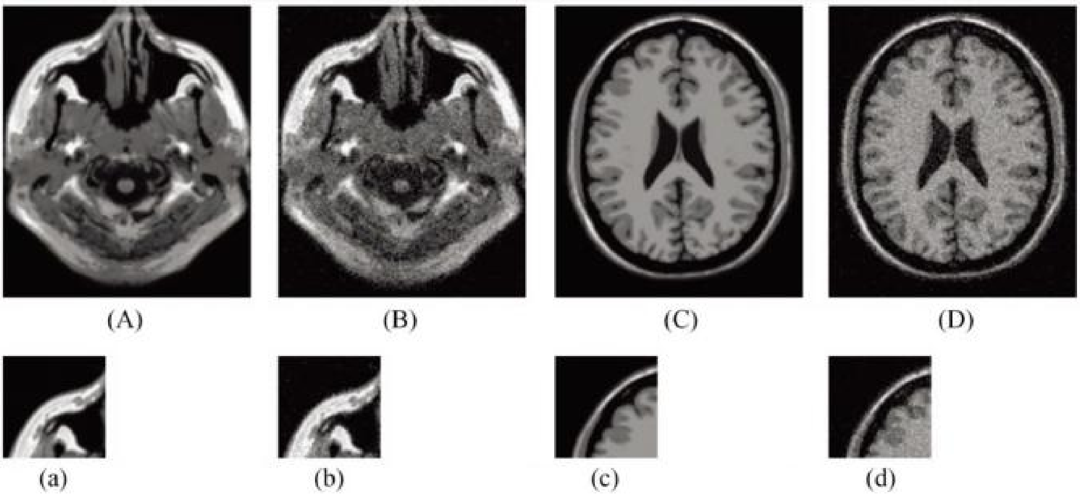

Figure 2: Synthetic MR data (Longitudinal relaxation time) obtained from the SBD for Experiment.

2.1 Unraveling Representation

In the unsupervised domain, because the data is not paired [23] [24] [25],separating the content information from the noise information in the images poses a challenge for us.. This paper improves the separation of content information and noise information in noisy images from two aspects. On one hand, we extract as much effective content information as possible from the low-quality images. Since high-quality images are not affected by noise, Ech can extract content information without noise. To better extract content information from low-quality images, we adopt a strategy of sharing weight parameters between ECL and ECH . On the other hand, we constrain the distribution of noise features Zn by adding KL divergence loss, making it approximately a normal distribution. The KL divergence loss is shown in Equation (1).

$$\boldsymbol{KL}\big(\boldsymbol{q}(\boldsymbol{z_N})|\boldsymbol{p}(\boldsymbol{z})\big) =- \int \boldsymbol{q}(\boldsymbol{z_N}) \, \mathbf{log}_{\boldsymbol{q}(\boldsymbol{z_N})} \, \mathrm{d}\, \boldsymbol{z} \tag{1}$$

The minimization of KL divergence and Equation (2) are equivalent.

$$\boldsymbol{L_{KL}} = \frac{\mathbf{1}}{\mathbf{2}} \sum_{\boldsymbol{i}=\mathbf{1}}^{\boldsymbol{N}} \left(\boldsymbol{\mu}_{\boldsymbol{i}}^{\mathbf{2}} + \boldsymbol{\sigma}_{\boldsymbol{i}}^{\mathbf{2}} - \mathbf{log}\left(\boldsymbol{\sigma}_{\boldsymbol{i}}^{\mathbf{2}}\right) - \mathbf{1} \right) \tag{2}$$

2.2 Loss due to adversarial components

To enhance the generation of realistic high-quality images, we employ adversarial loss within both domains[22], as shown in Equation (3).

$$L_{Dh} = E_{h\sim p(h)}[\log D_H\,(h)] + E_{l\sim p(l)}\left[\log\left(1 - D_H(\text{ fakeh })\right)\right] \tag{3}$$

fakeh is defined as shown in Equation (4).

$$\text{fakeh } = G_H(E_L^c(l), z_N) \tag{4}$$

During the training process, HG tries to make the generated image fakeh look more similar to the images from the high-quality image domain, while HD aims to distinguish fakeh from real samples h. GH wants to minimize the loss as much as possible during training, while DH wants to maximize the loss. The adversarial loss in the low-quality image domain is specified in Equation(5).

$$L_{Dl} = E_{l\sim p(l)}[\log D_L\,(l)] + E_{h\sim p(h)}\left[\log\left(1 - D_L(\text{ fakel })\right)\right] \tag{5}$$

fakeh is defined as shown in Equation (4).

$$\text{fakel } = G_L(E_H^c(h), z_N) \tag{6}$$

2.3 Cycle Consistency Loss

Under unsupervised conditions, only adversarial loss cannot guarantee the consistency of content information. Taking inspiration from CycleGAN [22], we incorporated cycle consistency loss into the model, as depicted in Equation(7).

$$L_{cyc} = E_{h\sim p(h)}[|h - \text{ fakeh } h|_1] + E_{l\sim p(l)}[|l - \text{ fakell } |_1] \tag{7}$$

In Section 2.2, we generated fakel and fakeh. In this section, we need to regenerate the input fakel into an image in the high-quality domain. The reconstructed high-quality image is defined as shown in Equation (8).

$$\text{fakehh } = G_H\big(E_L^c(\text{ fakel }), E^n(\text{ fakel })\big) \tag{8}$$

Similarly, we reconstruct fakeh into the original low-quality domain image. The reconstructed low-quality image is defined as shown in Equation (9).

$$\text{fakell } = G_L\big(E_H^c(\text{ fakeh }), E^n(\text{ fakel })\big) \tag{9}$$

2.4 KL Divergence Loss

We aim for the generated image fakel to only contain the noise information from the image l. However, the actual experimental results do not align with our expectations. In fact, due to incomplete separation, the generated fakel also contains content information from the image l. To improve the generation of fakel, we further constrain the model using perceptual loss. The perceptual loss is defined as shown in Equation (10).

$$L_{pe} = |fe_{l-\text{ layer}}(\text{ fakel }) - fe_{l-\text{ layer}}(l)|_2^2 \tag{10}$$

$\boldsymbol{fe_{l-\text{ layer}}(x)}$ represents the feature of a pre-trained convolutional neural network [26].

The model's objective function is described as shown in Equation (11):

$$\text{Loss } = \boldsymbol{\lambda_{Dhl}(L_{Dh} + L_{Dl}) + \lambda_{KL}L_{KL} + \lambda_{cyc}L_{cyc} + \lambda_{pe}L_{pe}} \tag{11}$$

Given the noisy MRI image lt, we need to input it into GH to obtain a high-quality image, as shown in Equation (12):

$$\boldsymbol{deimg = G_H\left(E_L^c(l_t), E^n(l_t)\right)} \tag{12}$$

3. 3. EXPERIMENTAL RESULTS

To assess the effectiveness of our proposed model, we conducted a comparative analysis with the classical image denoising method Anisotropic Diffusion Filter (ADF) and the unsupervised image denoising approach CycleGAN based on deep learning. The experiments were performed using synthetic MRI data (Longitudinal relaxation time and PDw) acquired from SBD. The test data included Longitudinal relaxation time and PDw images with Rician noise levels of 5%, 10%, 15%, 20%, 25%, and 30%.

Figures 3 to 8 present the experimental results for the Longitudinal relaxation time images, and from the comparison, it is evident that our denoising method achieved good visual results. As the Rician noise intensity increased, the denoising results from ADF increasingly contained noticeable noise. When the noise intensity exceeded 20%, the residual noise significantly affected the visual performance.

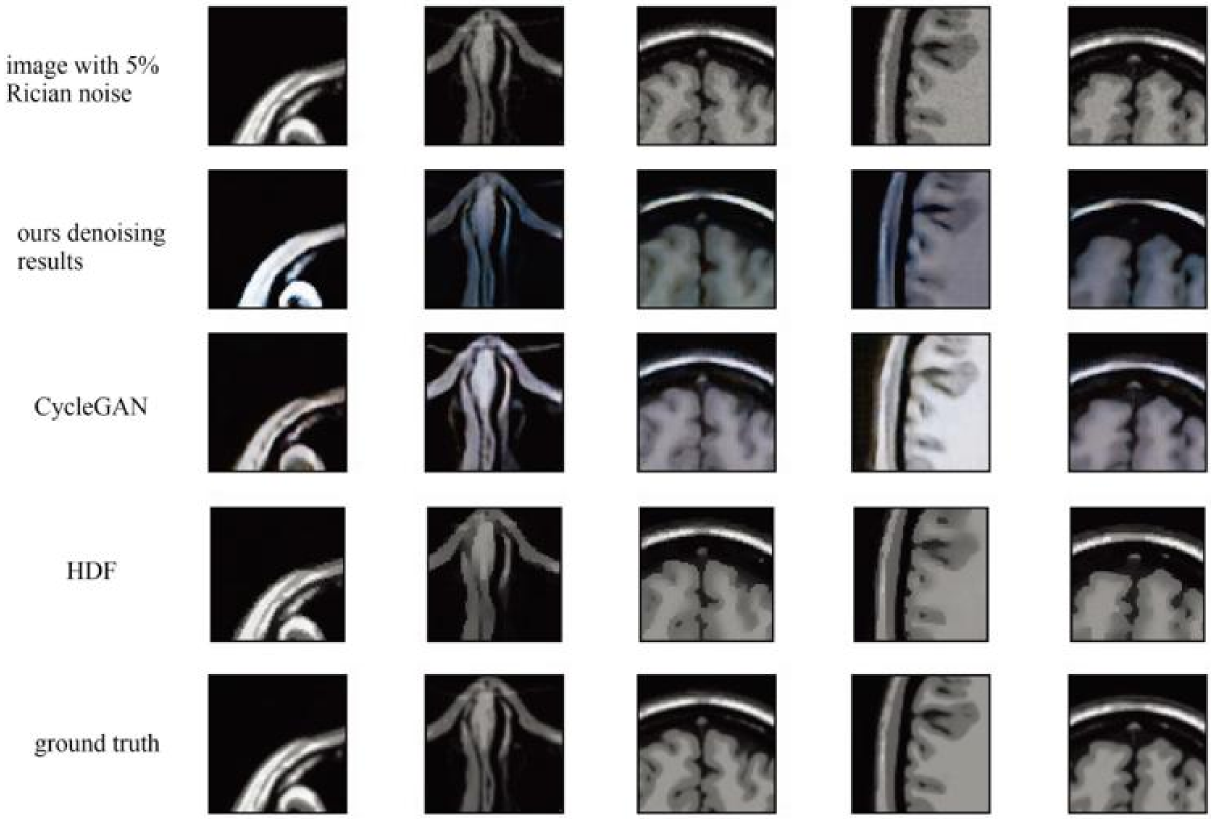

Figure 3: Conducting an experiment on the Longitudinal relaxation time image with 5% Rician noise.

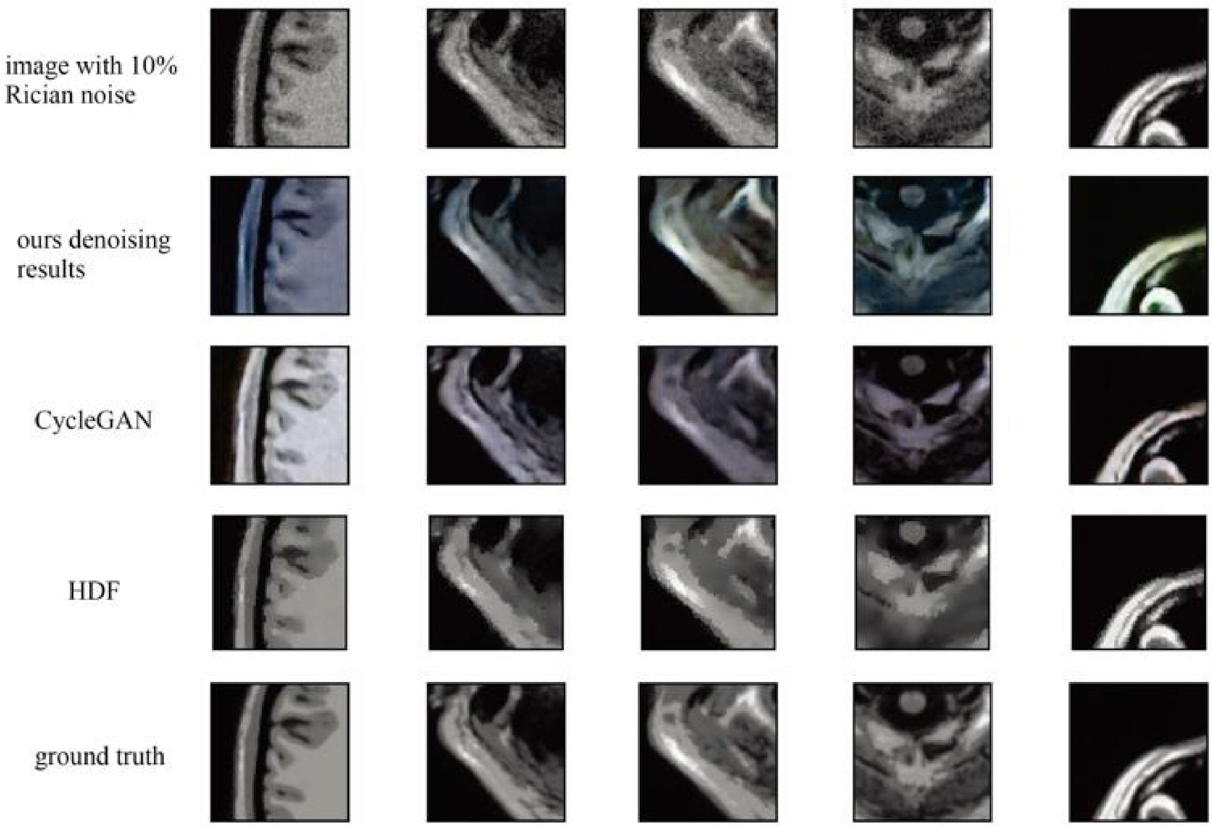

Figure 4: Conducting an experiment on the Longitudinal relaxation time image with 10% Rician noise.

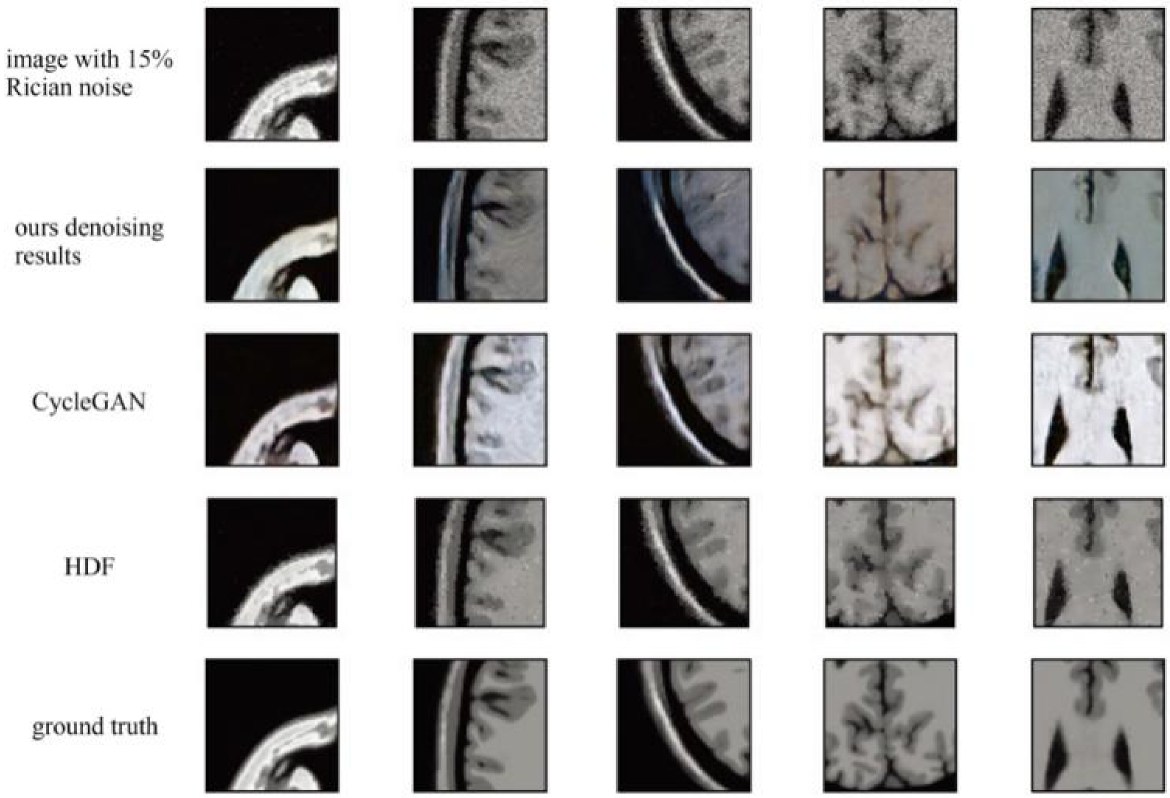

Figure 5: Conducting an experiment on the Longitudinal relaxation time image with 15% Rician noise.

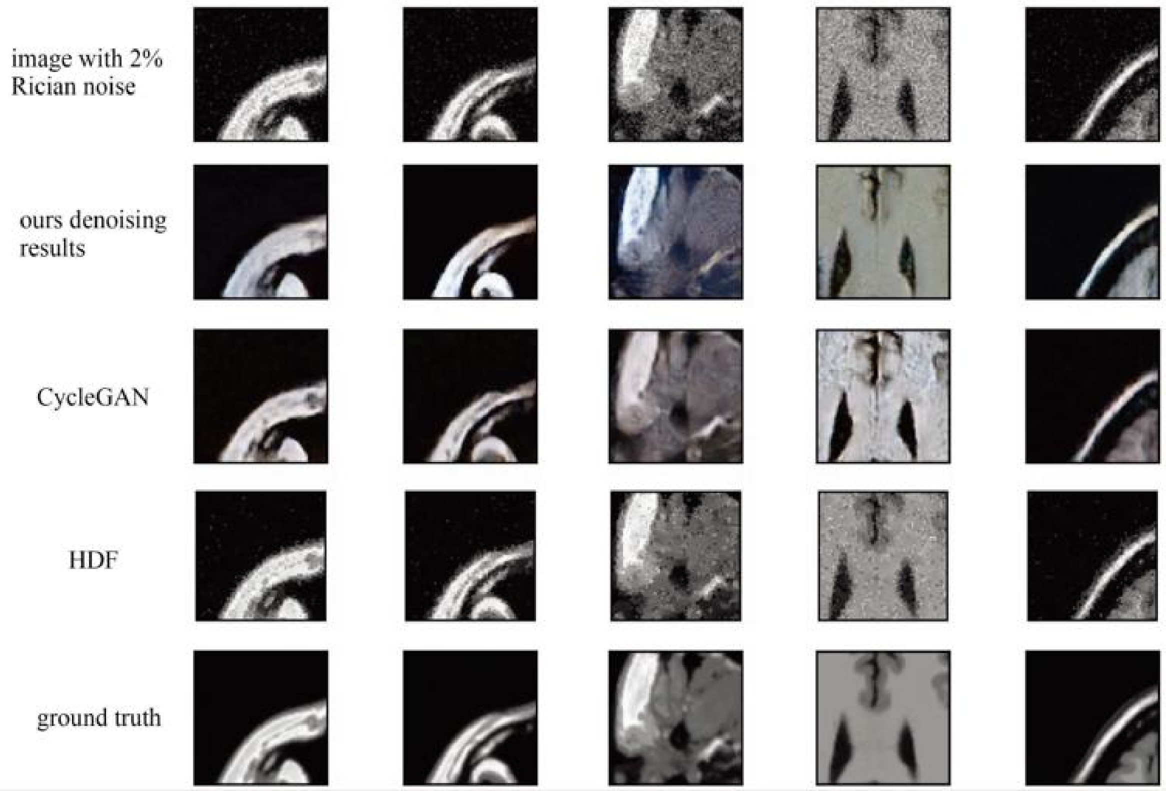

Figure 6: Conducting an experiment on the Longitudinal relaxation time image with 20% Rician noise.

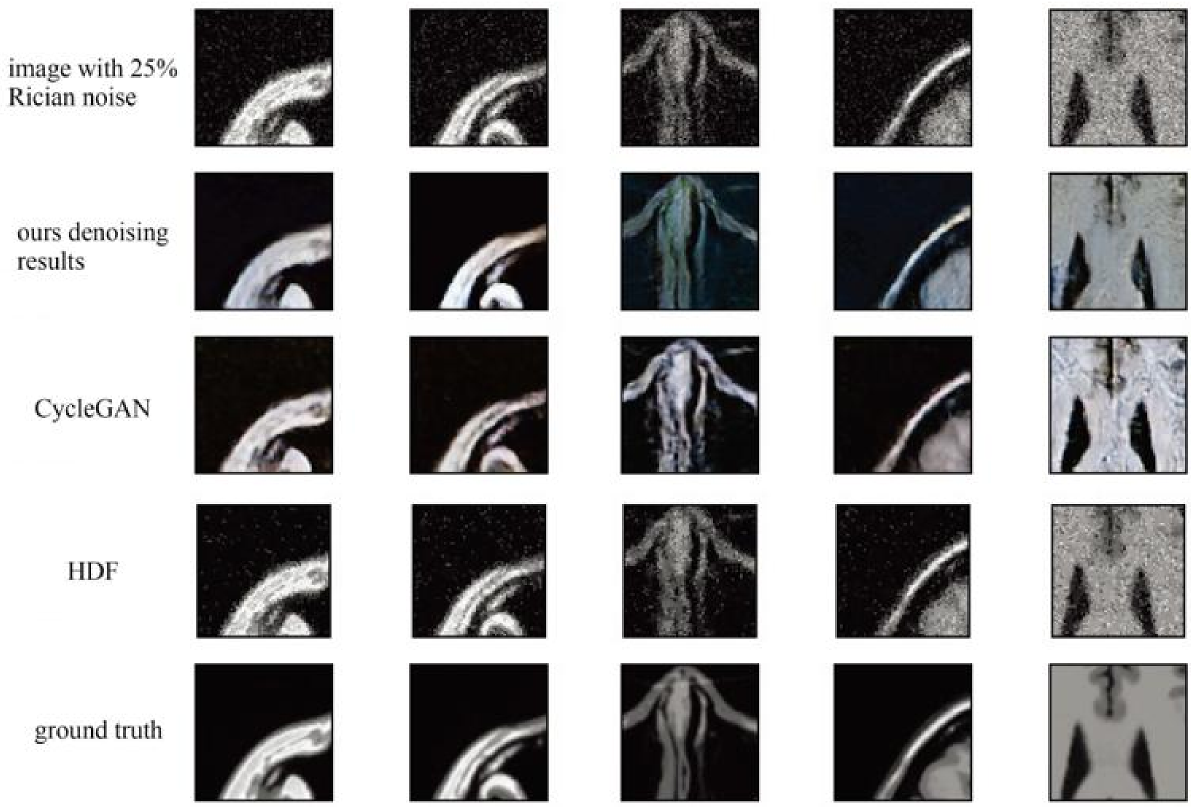

Figure 7: Conducting an experiment on the Longitudinal relaxation time image with 25% Rician noise.

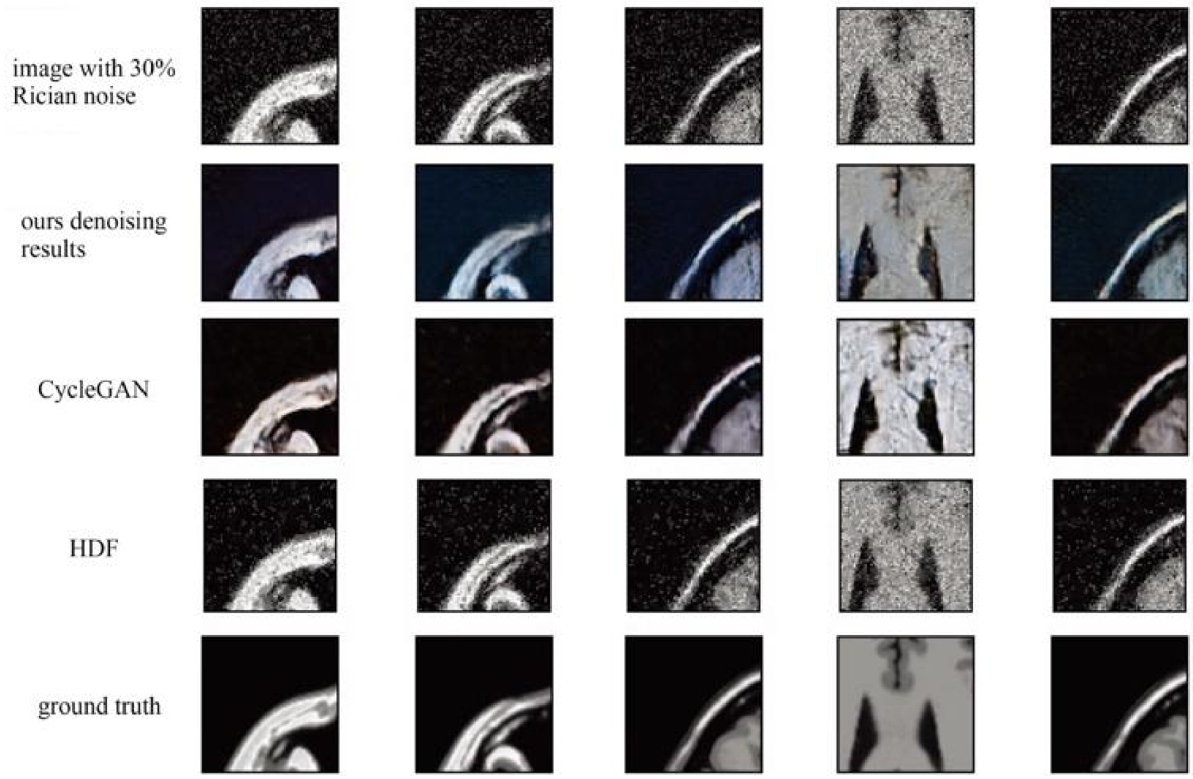

Figure 8: Conducting an experiment on the Longitudinal relaxation time image with 30% Rician noise.

As shown in Table 1, the SSIM and PSNR of the ADF algorithm are lower than those of CycleGAN and our proposed method. Our proposed algorithm achieved higher PSNR values compared to the other methods when the noise level was below 25%. When the noise intensity increased to 30%, CycleGAN exhibited a slightly superior PSNR value compared to our algorithm. However, our proposed algorithm still obtained competitive SSIM values, as shown in Table 2.

Table 1: Our algorithm's PSNR value was slightly surpassed by that of CycleGAN.

METHOD	5%	10%	15%	20%	25%	30%
ADF	20.5106	20.2641	19.9734	18.8793	17.8912	16.7202
CycleGAN	20.1260	20.0429	20.1983	20.0368	20.0532	19.6573
Ours	22.4934	22.3121	22.2458	21.3219	20.3421	19.5304

Table 2: SSIM outcomes for different techniques applied to the Longitudinal relaxation time image under various Rician noise levels.

Method	5%	10%	15%	20%	25%	30%
ADF	0.7234	0.7201	0.6231	0.5123	0.3814	0.3014
CycleGAN	0.7206	0.7342	0.6311	0.6207	0.5887	0.5301
Ours	0.7592	0.7123	0.6679	0.6021	0.5443	0.4894

4. CONCLUSION

The removal of noise from inferior-quality MRI images to obtain superior-quality MRI images is of considerable importance. This paper introduces an unsupervised image denoising algorithm based on generative adversarial networks. In the context of rapid advancements in Artificial Intelligence, especially in fields such as Bioinformatics[27][28][29], we are witnessing a significant increase in the integration of Artificial Intelligence in healthcare. This trend is also observable in the realm of computer vision [30][31]. The model disentangles the content information and noise information of the noisy image through a disentangled representation and regularizes the noise distribution using KL divergence loss. The model employs perceptual loss and cycle-consistency loss to ensure consistency of content information. Moreover, adversarial loss is incorporated into the model to generate more realistic MRI images. The experimental results illustrate that our proposed method achieves effective denoising effects.

Due to the relatively large number of parameters in this model, it requires certain specifications for the training platform. Therefore, we plan to optimize the network structure to reduce the number of model parameters without compromising the denoising performance.

REFERENCES

[1] Buades, A., Coll, B. and Morel, J.-M. (2005) A Non-Local Algorithm for Image Denoising. 2005 IEEE Computer Society Conference on Computer Vision and Pattern Recognition (CVPR'05), San Diego, 20-25 June 2005, 60-65.

[2] Manjón, J.V., Carbonell-Caballero, J., A, Lull, J.J., García-Martí, G., Martí-Bonmatí, L. and Robles, M. (2008) MRI Denoising Using Non-Local Means. Medical Image Analysis, 12, 514-523. https://doi.org/10.1016/j.media.2008.02.004

[3] Dabov, K., Foi, A., Katkovnik, V. and Egiazarian, K. (2007) Image Denoising by Sparse 3-D Transform-Domain Collaborative Filtering. IEEE Transactions on Image Processing, 16, 2080-2095. https://doi.org/10.1109/TIP.2007.901238

[4] Eksioglu, E.M. (2016) Decoupled Algorithm for MRI Reconstruction Using Nonlocal Block Matching Model: BM3D-MRI. Journal of Mathematical Imaging & Vision, 56, 430-440. https://doi.org/10.1007/s10851-016-0647-7

[5] Weinan Dai, Chengjie Mou, Jun Wu, and Xuesong Ye. 2023. Diabetic Retinopathy Detection with Enhanced Vision Transformers: The Twins-PCPVT Solution. In 2023 IEEE 3rd International Conference on Electronic Technology, Communication and Information (ICETCI). IEEE, 403–407.

[6] Hao Xu, Shuang Song, and Ze Mao. 2023. Characterizing the Performance of Emerging Deep Learning, Graph, and High Performance Computing Workloads Under Interference. arXiv:2303.15763

[7] Zhang, Y., Yang, Z., Hu, J., Zou, S. and Fu, Y. (2019) MRI Denoising Using Low Rank Prior and Sparse Gradient Prior. IEEE Access, 7, 45858-45865. https://doi.org/10.1109/ACCESS.2019.2907637

[8] Chang Che, Bo Liu, Shulin Li, Jiaxin Huang, and Hao Hu. 2023. Deep Learning for Precise Robot Position Prediction in Logistics. Journal of Theory and Practice of Engineering Science 3, 10 (Oct. 2023), 36–41. https://doi.org/10.53469/jtpes. 2023.03(10).05

[9] Szegedy, C., Liu, W., Jia, Y., Sermanet, P., Reed, S., Anguelov, D., Erhan, D., Vanhoucke, V. and Rabinovich, A. (2015) Going Deeper with Convolutions. Proceedings of the IEEE Conference on Computer Vision and Pattern Recognition, Boston, 7-12 June 2015, 1-9. https://doi.org/10.1109/CVPR.2015.7298594

[10] SiYuan Cheng, BinFei Chu, BiNeng Zhong, ZiKai Zhang, Xin Liu, ZhenJun Tang, and XianXian Li. 2021. DRNet: Towards fast, accurate and practical dish recognition. Science China Technological Sciences 64, 12 (2021), 2651–2661.

[11] Zichen Liang, Hu Cao, Chu Yang, Zikai Zhang, and Guang Chen. 2022. Global local feature aggregation for event-based object detection on eventkitti. In 2022 IEEE International Conference on Multisensor Fusion and Integration for IntelligentInvestigation of Creating Accessibility Linked Data Based on Publicly Available Accessibility Datasets CCNS, December 1-3, 2023, Fuzhou, China Systems (MFI). IEEE, 1–7.

[12] Jiang, D., Dou, W., Vosters, L., et al. (2018) Denoising of 3D Magnetic Resonance Images with Multi-Channel Residual Learning of Convolutional Neural Network. Japanese Journal of Radiology, 36, 566-574. https://doi.org/10.1007/s11604-018-0758-8

[13] Manjón, J.V. and Coupé, P. (2018) MRI Denoising Using Deep Learning. In: Bai, W., Sanroma, G., Wu, G., Munsell, B., Zhan, Y. and Coupé, P., Eds., International Workshop on Patch-Based Techniques in Medical Imaging, Springer, Cham, 12-19. https://doi.org/10.1007/978-3-030-00500-9_2

[14] Abbasi, A., Monadjemi, A., Fang, L., Rabbani, H. and Zhang, Y. (2019) Three-Dimensional Optical Coherence Tomography Image Denoising through Multi-Input Fully-Convolutional Networks. Computers in Biology and Medicine, 108, 1-8. https://doi.org/10.1016/j.compbiomed.2019.01.010

[15] Hao Xu, Qingsen Wang, Shuang Song, Lizy Kurian John, and Xu Liu. 2019. Can we trust profiling results? Understanding and fixing the inaccuracy in modern profilers. In Proceedings of the ACM International Conference on Supercomputing. 284–295.

[16] Radford, A., Metz, L. and Chintala, S. (2015) Unsupervised Representation Learning with Deep Convolutional Generative Adversarial Networks. arXiv preprint arXiv:1511.06434.

[17] Arjovsky, M., Chintala, S. and Bottou, L. (2017) Wasserstein Gan. arXiv preprint arXiv:1701.07875.

[18] Chen, J., Chen, J., Chao, H. and Yang, M. (2018) Image Blind Denoising with Generative Adversarial Network Based Noise Modeling. 2018 IEEE/CVF Conference on Computer Vision and Pattern Recognition (CVPR), Salt Lake City, 18-23 June 2018, 3155-3164. https://doi.org/10.1109/CVPR.2018.00333

[19] Yeh, R.A., Lim, T.Y., Chen, C., Schwing, A.G., Hasegawa-Johnson, M. and Do, M. (2018) Image Restoration with Deep Generative Models. 2018 IEEE International Conference on Acoustics, Speech and Signal Processing (ICASSP), Calgary, 15-20 April 2018, 6772-6776. https://doi.org/10.1109/ICASSP.2018.8462317
[20] Lu, S., Lu, Z. and Zhang, Y.D. (2019) Pathological Brain Detection Based on AlexNet and Transfer Learning. Journal of Computational Science, 30, 41-47. https://doi.org/10.1016/j.jocs.2018.11.008
[21] Lu, S., Wang, S.H. and Zhang, Y.D. (2020) Detection of Abnormal Brain in MRI via Improved AlexNet and ELM Optimized by Chaotic Bat Algorithm. Neural Computing and Applications. https://doi.org/10.1007/s00521-020-05082-4
[22] Zhu, J.Y., Park, T., Isola, P. and Efros, A.A. (2017) Unpaired Image-to-Image Translation Using Cycle-Consistent Adversarial Networks. 2017 IEEE International Conference on Computer Vision (ICCV), Venice, 22-29 October 2017, 2242-2251. https://doi.org/10.1109/ICCV.2017.244
[23] Hao Hu, Shulin Li, Jiaxin Huang, Bo Liu, and Chang Che. 2023. Casting Product Image Data for Quality Inspection with Xception and Data Augmentation. Journal of Theory and Practice of Engineering Science 3, 10 (Oct. 2023), 42–46. https: //doi.org/10.53469/jtpes.2023.03(10).06
[24] Chengjie Mou, Xuesong Ye, Jun Wu, and Weinan Dai. 2023. Automated ICD Coding Based on Neural Machine Translation. In 2023 8th International Conference on Cloud Computing and Big Data Analytics (ICCCBDA). IEEE, 495–500.
[25] Hao Xu, Min Zhu, and Yan-Bo Wu. 2014. An algorithm of multi-array Turbo equalization of underwater acoustic communication. Journal of Electronics Information Technology 36, 6 (2014), 1465–1471.
[26] Zikai Zhang, Bineng Zhong, Shengping Zhang, Zhenjun Tang, Xin Liu, and Zhaoxiang Zhang. 2021. Distractor-aware fast tracking via dynamic convolutions and mot philosophy. In Proceedings of the IEEE/CVF conference on computer vision and pattern recognition. 1024–1033.
[27] Weinan Dai, Yifeng Jiang, Chengjie Mou, and Chongyu Zhang. 2023. An Integrative Paradigm for Enhanced Stroke Prediction: Synergizing XGBoost and xDeepFM Algorithms. In Proceedings of the 2023 6th International Conference on Big Data Technologies (ICBDT '23). Association for Computing Machinery, New York, NY, USA, 28–32. https://doi.org/10.1145/3627377.3627382
[28] C. Mou, W. Dai, X. Ye and J. Wu, "Research On Method Of User Preference Analysis Based on Entity Similarity and Semantic Assessment," 2023 8th International Conference on Signal and Image Processing (ICSIP), Wuxi, China, 2023, pp. 1029-1033, doi: 10.1109/ICSIP57908.2023.10271084.
[29] Xuesong Ye, Jun Wu, Chengjie Mou, and Weinan Dai. 2023. MedLens: Improve Mortality Prediction Via Medical Signs Selecting and Regression. In 2023 IEEE 3rd International Conference on Computer Communication and Artificial Intelligence (CCAI). IEEE, 169–175.
[30] Jun Wu, Xuesong Ye, Chengjie Mou, and Weinan Dai. 2023. Fineehr: Refine clinical note representations to improve mortality prediction. In 2023 11th International Symposium on Digital Forensics and Security (ISDFS). IEEE, 1–6.
[31] Tianbo, Song, Hu Weijun, Cai Jiangfeng, Liu Weijia, Yuan Quan, and He Kun. "Bio-inspired Swarm Intelligence: a Flocking Project With Group Object Recognition." In 2023 3rd International Conference on Consumer Electronics and Computer Engineering (ICCECE), pp. 834-837. IEEE, 2023.